Changes in Liposome Morphology Induced by Actin Polymerization in Submicrometer Liposomes

ARTICLE *in* LANGMUIR · NOVEMBER 2003

Impact Factor: 4.46 · DOI: 10.1021/la035114d

2 AUTHORS, INCLUDING:

Jonathan D Nickels
Oak Ridge National Laboratory
45 PUBLICATIONS **549** CITATIONS

Changes in Liposome Morphology Induced by Actin Polymerization in Submicrometer Liposomes

Jonathan Nickels and Andre F. Palmer*

Department of Chemical and Biomolecular Engineering, University of Notre Dame, Notre Dame, Indiana 46556

Received June 23, 2003. In Final Form: October 8, 2003

A morphological change in actin-containing liposomes produced via extrusion across a 400 nm pore diameter polycarbonate membrane in low ionic strength buffer (G-buffer) is induced by the addition of high ionic strength buffer (F-buffer). The change in conformation is due to the polymerization of monomeric G-actin within the inner compartment of the liposome and the subsequent deformation of the initially spherical liposome into a disklike geometry. This result was elucidated by applying various form factors corresponding to different geometries to light scattering data derived from actin-containing liposome dispersions. The results of this analysis showed that empty (no actin) liposomes in G-buffer and F-buffer, as well as actin-containing liposomes in G-buffer, were all spherelike objects between 250 and 450 nm in diameter, depending on osmotic conditions. The findings further showed that the actin-containing liposomes in F-buffer took on a thin, disklike shape, a result of the internal polymerization of the actin monomers into filaments.

Introduction

The cell cytoskeleton plays an important role during cellular remodeling processes such as cell motility, cytokinesis, pinocytosis, and phagocytosis.[1,2] Hence, a detailed understanding of how the cytoskeleton coupled to the surrounding cell membrane determines cell shape during these dynamic processes is critical, to understand how these processes function. Although liposomes have been widely used to study many aspects of eukaryotic cell function such as aggregation, fusion, and selective permeability,[2−4] plain liposomes do not present a suitable model for studying the interaction between lipid bilayers and cytoskeletal networks due to the absence of an internal scaffold.

The cytoskeleton is composed primarily of three structural proteins: actin, tubulin, and keratin, along with various other regulatory proteins.[1] In this work, we studied changes in liposome morphology associated with the introduction of an artificial actin cytoskeleton. The actin molecule itself has been thoroughly characterized.[5] The inclusion of actin in liposomes is not, however, a new idea. Existing works have illuminated many phenomena on the topic. Several groups have successfully encapsulated actin into giant liposomes. The diameter of these giant liposomes was typically on the order of ∼10 microns, to mimic the size of an actual eukaryotic cell.

Miyata and Hotani[6] were one of the first groups to successfully encapsulate actin within giant liposomes. The initially spherically shaped liposomes deformed into both dumbbell or disk geometries due to actin polymerization. In a subsequent study by Miyata et al.,[7] transient pores were created in the liposome membrane by electroporation. This permitted KCl in the bulk solution to diffuse into the aqueous core of the liposome through the transient pores, which polymerized the G-actin. In this case, thin protrusive invaginations consisting of actin filaments encased in a lipid bilayer extended from the surface of the initially spherical liposome surface.

Using an AC field, Häckl et al.[8] created a monodisperse population of spherical giant actin-containing liposomes in high yield. Polymerization was induced by the addition of Mg^{2+} ions, which diffused into the liposome aqueous core through Mg^{2+} ion channels that were imbedded in the lipid bilayer, thus polymerizing the G-actin. The resultant giant actin liposome retained its spherical shape. However, a thin actin shell or cortex developed around the inside leaflet of the giant liposome.

Boulbitch et al.[9] also studied giant liposomes with an underlying actin cortex and showed that the presence of this cortex triggered local shape instabilities in the associated lipid bilayer membrane, forming blisters when the temperature was slightly increased. In an extension of the previously mentioned study, Helfer et al.[10] studied a self-assembled network of actin filaments attached to the outer surface of giant liposomes and found that the presence of this network strongly modified the membrane dynamics from that seen with an uncoated lipid bilayer.

This work focuses on the morphological change that occurs when a liposome containing G-actin in low ionic strength buffer (G-buffer) is exposed to high ionic strength buffer (F-buffer) thereby causing actin polymerization. This was done with liposomes with a hydrodynamic radius of ∼200 nm in G-buffer before addition of 10× F-buffer in a 1:9 volume ratio. The fundamental difference between our study and the previously mentioned studies is that the diameter of our actin-containing liposomes is small, ∼400 nm, compared to that of a typical giant liposome,

* Corresponding author.

(1) Lodish, H.; Berk, A.; Zipursky, S.; Matsudaira, P.; Baltimore, D.; Darnell, J. W. H. Freeman: New York, 1999.
(2) Staunch, O.; Uhlmann, T.; Fröhlich, M.; Thomann, R.; El-Badry, M.; Kim, Y.-K.; Schubert, R. *Biomacromolecules* **2002**, *3*, 324−332.
(3) Jass, J.; Tjärnhage, T.; Puu, G. *Biophys. J.* **2000**, *79*, 3153−3163.
(4) Teschke, O. *Langmuir* **2002**, *18*, 6513−6520.
(5) Pollard, T. D.; Cooper, J. A. *Annu. Rev. Biochem.* **1986**, *55*, 987−1035.
(6) Miyata, H.; Hatani, H. *Biophysics* **1992**, *89*, 11547−11551.
(7) Miyata, H.; Nishiyama, S.; Akashi, K.; Kinosita, K., Jr. *Proc. Natl. Acad. Sci. U.S.A.* **1999**, *96*, 2048−2053.
(8) Häckl, W.; Bärmann, M.; Sackmann, E. *Phys. Rev. Lett.* **1998**, *80*, 1786−1789.
(9) Boulbitch, A.; Simson, R.; Simson, D. A.; Merkel, R.; Häckl, W.; Bärmann, M.; Sackmann, E. *Phys. Rev. E.* **2000**, *62*, 3974−3985.
(10) Helfer, E.; Harlepp, S.; Bourdieu, L.; Robert, J.; MacKintosh, F. C.; Chatenay, D. *Phys. Rev. E* **2001**, *63*, 021904-1-13.

10.1021/la035114d CCC: $25.00
Published on Web 11/13/2003

~10 microns. In our study, we want to investigate the effect of confinement on the resultant actin-containing liposome three-dimensional structure. We will determine the shape of these actin-containing liposome dispersions using asymmetric flow field-flow fractionation (AFFF) coupled with multi-angle static light scattering (MASLS). Investigations on the morphology of giant liposomes were exclusively measured using optical microscopy. To our knowledge, AFFF coupled with MASLS has not been previously used to study the morphology of these actin-containing liposome dispersions.

Experimental Section

Chemicals. L-α-Phosphatidylcholine (PC) derived from egg-yolk tissue with >99% purity was obtained from Avanti Polar Lipids (Alabaster, AL) and stored in chloroform stock solutions at −20 °C. Monomeric actin, G-buffer (5 mM Tris−HCl, pH 8.0, 0.2 mM $CaCl_2$, and 0.2 mM ATP), and F-buffer (50 mM KCl, 2 mM $MgCl_2$, and 1mM ATP) were obtained from Cytoskeleton (Denver, CO). K^+ ionophore was obtained from Fluka (Buchs, Switzerland). All water was taken from a Barnstead E-Pure (Barnstead/Thermolyne, Dubuque, IA) ultrapure water system with a resistivity of 18.1 MΩ cm and filtered through 0.02 μm inorganic membrane filters obtained from Whatman (Maidstone, U.K.).

G-Buffer was used for all MASLS studies of plain liposomes and liposomes encapsulating G-actin. F-buffer was used for all studies of plain liposomes and liposomes encapsulating G-actin under polymerizing conditions.

Asymmetric Flow Field-Flow Fractionation Coupled with Multi-angle Light Scattering. An asymmetric flow field-flow fractionator (Eclipse) connected in series with a MASLS photometer (Dawn Eos) (Wyatt Technologies, Santa Barbara, CA) was used to measure the shape and geometric dimensions of plain liposomes and liposomes encapsulating actin. During a typical experiment, the liposome dispersion is injected into the AFFF channel, where it is separated. The separated liposome dispersion eluent then flows into the MASLS photometer, which continuously measures the particles' size and shape as a function of time.

The multiangle laser photometer is temperature-controlled to within 0.1 °C and was maintained at 25 °C for all MASLS measurements. The photometer is equipped with a 30 mW gallium-arsenide diode laser that emits a vertically polarized beam with a wavelength of 690 nm *in vacuum*, which is scattered by the sample. The scattered light is collimated and simultaneously detected by a fixed array of 18 transimpedance photodiodes, which span an angular region from 22.5° to 147°. The light scattering intensity profile was recorded as a function of time at a rate of one full profile every second. Here, $Q = (4\pi n/\lambda_0)\sin(\theta/2)$ is the amplitude of the scattering wave vector, $n = 1.3316$ is the refractive index of the buffer solution, θ is the scattering angle, and $\lambda_0 = 690$ nm is the wavelength of the incident light beam in a vacuum. In preparation for all AFFF/MASLS experiments, all glassware was carefully cleaned, while all mobile phases (G- and F-buffer) were thoroughly filtered through 0.1 micron filters.

Asymmetric flow field-flow fractionation is a chromatographic separation technique, which is capable of separating a dispersion of polydisperse particles with sizes ranging from 1 nm to 10 microns, using two orthogonal flow fields acting within a trapezoidal shaped channel. The top of the channel is bounded by an optically transparent acrylic block, while the bottom is bounded by a 10 000 molecular weight cutoff polymeric membrane, Nadir (Millipore, USA). For all experiments, the channel height was fixed at 350 microns. One flow field, the channel flow (v_c), is parallel to the polymer membrane. The other flow field, the cross flow (v_x), is perpendicular to the membrane.

In the focus/inject mode of operation, the liposome dispersion is injected into the channel, where it is subjected to a cross flow of 3 mL/min and a channel flow of 0 mL/min for 3 min. Liposomes exposed to the cross flow accumulate toward the membrane surface, where they rapidly equilibrate via molecular diffusion and form a thin ellipsoidal sample front. The ellipsoidal sample front is perpendicular to the channel flow. In the elution mode of operation, the ellipsoidal sample region is exposed to a channel flow of 1 mL/min and a cross flow of 1.5 mL/min, which linearly decreases to 0 mL/min in a 30 min interval. The cross flow acts to retain particles longer in the channel, thus separating the dispersion based on particle size.

In a typical separation, small particles (<1 micron) elute from the channel first, while larger particles elute last. This is characterized by an exponential distribution of particles near the accumulation wall (membrane). In the hyperlayer mode of operation, the elution order is reversed. In this case, particles with diameters larger than ~1 micron elute first. For the experiments described in this paper, a typical separation lasted 60 min.

Liposome, Actin, and Substrate Preparation. Liposomes were prepared by extrusion in stainless steel−Teflon extruders using 0.4 micron polycarbonate membranes, all obtained from Avanti Polar Lipids (Alabaster, AL). The extrusion procedure has been described well elsewhere.[11−14] In short, 0.01 volume of K^+ ionophore dissolved in chloroform (25 mg/mL) was added to 0.99 volume of 20 mg/mL PC, also dissolved in chloroform. This solution was dried in a round-bottom flask by rotary evaporation of the solvents at 40 °C for 4 h, to ensure complete removal of chloroform. The resultant dried PC/ionophore film was rehydrated in either G-buffer (for liposomes not containing actin) or in a solution of 0.4 mg G-actin dissolved in 745 μL of G-buffer plus 255 μL of deionized H_2O (for liposomes containing actin).

Before liposome extrusion, rehydrated PC/ionophore solutions were vortexed vigorously for ~10 min to ensure even mixing. The aqueous lipid solutions were then extruded 15 times back and forth through the membrane, to yield plain liposomes and liposomes encapsulating G-actin. For liposomes encapsulating F-actin, polymerization was induced throughout the aqueous core of liposomes encapsulating G-actin by adding 0.1 volume of 10× F-buffer (500 mM KCl, 20 mM $MgCl_2$, and 10mM ATP) to 0.9 volume of PC/ionophore solution and pipetting gently for ~5 min. After gentle mixing with the pipet, this solution was allowed to polymerize for ~1 h so that K^+ ions could permeate through the ionophores embedded in the liposome membrane from the outside solution. In preparation for AFFF/MASLS studies, plain liposomes and liposomes encapsulating G- and F-actin were injected into the AFFF channel at 10× dilution using either G- or F-buffer as the mobile phase. All liposome suspensions were used immediately following their preparation.

Theory

Light Scattering. The excess Rayleigh ratio R_θ is a convenient way of expressing the light scattered by a solution of particles at a particular angle. The following expression represents the scattering due to particles, which is equal to the difference in scattering between the particles in solution and the buffer solution.

$$R_\theta = r^2 \frac{I_\theta - I_{\theta,\text{solvent}}}{I_0 V} \tag{1}$$

Here, r is the distance between the scattering volume and the detector, I_θ is the scattered intensity of the solution, $I_{\theta,\text{solvent}}$ is the scattered intensity of the solvent, I_0 is the intensity of the incident beam, and V is the volume of the scattering medium. This definition of R_θ is very robust since it corrects for any stray light present in the scattering volume along with any fluctuations in laser power. The determination of the molecular weight and size of a monodisperse system of particles can be derived from the

(11) Olson, F.; Hunt, C. A.; Szoka, F. C.; Vail, W. J.; Papahadjopoulos, D. *Biochim. Biophys. Acta* **1979**, *557*, 9−23.
(12) Hope, M. J.; Bally, M. B.; Webb, G.; Cullis, P. R. *Biochim. Biophys. Acta* **1985**, *812*, 55−65.
(13) New, R. R. C. *Liposomes*: *A Practical Approach*; Oxford University Press: Oxford, 1990.
(14) Korgel, B. A.; van Zanten, J. H.; Monbouquette, H. G. *Biophys. J.* **1998**, *74*, 3264−3272.

Table 1. Form Factors for Various Geometries[a]

geometry	form factor[b]
infinitely thin hollow shell	$P(Q) = \left(\frac{\sin(QR)}{QR}\right)^2$
infinitely thin rod	$P(Q) - \frac{2}{QL}\int_0^{QL} \frac{\sin(x)}{x}\,dx - \left(\frac{\sin(QL/2)}{QL/2}\right)^2$
infinitely thin disk	$P(Q) = \left(\frac{2}{Q^2R^2}\right)\left(1 - \frac{J_1(2RQ)}{RQ}\right)$
circular cylinder	$P(Q) = \int_0^{\pi/2}\left(\frac{\sin((QL/2)\cos(x))2J_1(QR\sin(x))}{(QL/2)\cos(x)QR\sin(x)}\right)^2 \sin(x)\,dx$

[a] R, vesicle radius; L, vesicle length; $J_1(x)$, Bessel function of the first order. [b] See van Zanten (ref 20) for more information.

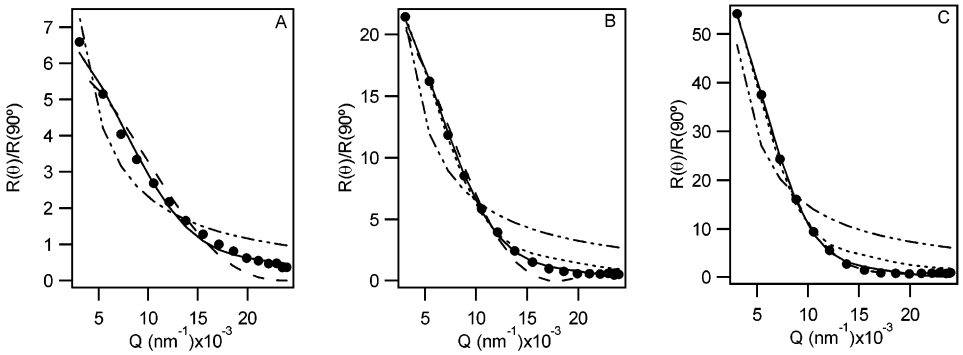

Figure 1. Light scattering spectra for plain liposomes in G-buffer at elution times of 35.317, 37.067, and 39.8 min shown in frames A−C, respectively. Experimental observations are represented by the solid dots (●). The solid line represents the cylinder fit (—), the dashed−double-dotted line the thin rod fits (−••), the dashed line the thin spherical shell fit (- -), and the dotted line the thin disk fit (•••). The thin disk fit overlaps the cylinder fit in part A.

following expression proposed by Zimm[15,16] for a vertically polarized monochromatic light source:

$$\frac{R}{Kc} = MP(\theta) - 2A_2cM^2P^2(\theta) \qquad (2)$$

Here, $K = 4\pi^2n^2(dn/dc)^2/(\lambda_0^4N_A)$ is the optical constant of the liposome solution, N_A is Avogadro's number which is equal to 6.023×10^{23}, c is the concentration of solute in solution, M is the molecular weight of the solute, $P(\theta)$ is the theoretically derived form factor which is a function of the size, shape, and structure of the particle, and A_2 is the second virial coefficient. Since Zimm's expression only takes into account single contacts between macromolecules, it is typically used to model particle scattering in dilute solutions.

This expression can be further simplified since the particle concentration and second virial coefficient are usually small numbers $\ll 1$. During the separation process, the concentration of liposomes is $\sim 10^{-6}$ mg/mL. Therefore, eq 2 is transformed into

$$\frac{R}{Kc} = MP(\theta) \qquad (3)$$

When analyzing MASLS spectra, the use of this equation is justified, since AFFF separates a polydisperse sample into monodisperse components, which then flow into and are measured by the MASLS photometer. Hence, for all intents and purposes, each eluting fraction is considered monodisperse.

To measure the size and shape of eluting liposomes, values of K and c are not needed. Instead, eq 3 can be normalized using the scattering from the 90° light scattering detector, $R(90°)$, to yield

$$\frac{R(\theta)}{R(90°)} \approx \frac{P(\theta)}{P(90°)} \qquad (4)$$

In our study, we fit the experimental MASLS spectra to the form factors listed in Table 1, to regress the characteristic dimensions for that particular geometry. Hence, we are able to deduce the shape and size of eluting liposomes by testing which shape factor provides the best fit to the experimental MASLS spectra.

Results

Plain Liposomes in G-Buffer and F-Buffer. Figure 1 shows the light scattering spectra for empty unilamellar L-α-phosphatidylcholine liposomes in G-buffer. The sample was prepared via extrusion across a 400 nm pore diameter membrane for 20 min (∼15 passes). The sample was then separated into monodisperse fractions using AFFF with the outlet stream passing directly into the MASLS photometer. The MASLS angular spectra were then used to obtain sizing parameters through nonlinear least-squares curve fitting to the form factors shown in Table 1. This plot shows the observed spectra as solid dots in comparison with the least-squares fits from the four form factors. Figure 1A−C shows the spectra compared with the least-squares fits at various times within the elution peak due to the fractionated components of the liposome dispersion. All three plots show that the cylindrical form factor (solid line) fit the experimental observations with a high degree of accuracy. In the early portions of the elution peak, however, the errors for the cylindrical fit are extremely large. This is due to the fact that the parameters derived from the cylinder fit collapse to infinite

(15) Zimm, B. *J. Chem. Phys.* **1948**, *16*, 1093−1099.
(16) Zimm, B. *J. Chem. Phys.* **1948**, *16*, 1099−1116.

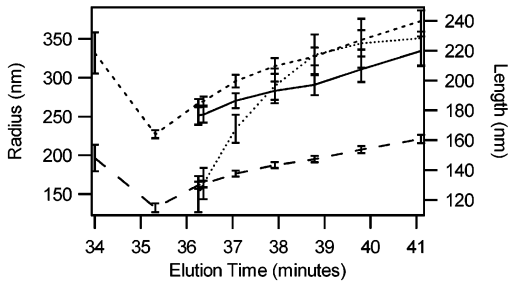

Figure 2. Physical sizing parameters for plain liposomes in G-buffer at eight representative times across the sample elution peak. Sizing parameters for three form factors are shown: the heavy dotted line represents the thin disk fit (•••), the dashed line represents the thin spherical shell fit (- -), and the cylinder fit is represented by the solid line (—) for its radial dimension and the lightly dotted line (···) for its length dimension (right axis).

thinness; however, it cannot obtain them due to a minimum length constraint placed on the fitting procedure, and this results in large errors.

This can be clearly seen in Figure 2, which shows the size parameters derived from the fits for the entire elution period. The thin spherical shell model also followed the trend of the experimental results, particularly in the lower Q ranges, and later elution times. The fitting procedure converged on radial sizes from ∼150 to ∼200 nm with parameter errors typically less than 2% or 3%. The thin rod form factor did not produce physically significant parameters. The thin disk form factor fit corresponded well to the experimental data only where the parameters derived from the cylinder fit collapsed to the same parameters derived from the thin disk model, as mentioned earlier. The cylinder fit yielded size parameters on the order of ∼250 to ∼300 nm radius and ∼140 to ∼225 nm length with errors of ∼5% to ∼10%. This analysis was conducted to provide a basis for comparison to the later work done with actin-containing liposomes; however, a complete control was also conducted for plain liposomes in F-buffer to allow for complete comparison.

Figure 3 shows the light scattering spectra for plain liposomes in F-buffer. The sample was prepared through the standard extrusion procedure across a 400 nm pore diameter membrane. Nonlinear least-squares fitting was again used to obtain fits for the four form factors. Panels A and B show the MASLS data with fits for two different elution times. This sample clearly shows that the thin spherical shell fits the experimental observations best at all times in the elution peak. Most other fits do however seem to approach the experimentally obtained values at high values of Q. The cylinder model, while distinct from the thin disk model, seemed to yield the next closest fit, while the thin rod model never seems to fit the data at any time or value of Q.

The sizing parameters for the cylinder, thin disk, and thin spherical shell fits are shown in Figure 4. The thin spherical shell fit predicts radial sizes of ∼50 to ∼125 nm with an error of ±5%. This seems small for a liposome produced by extrusion through a 400 nm diameter pore; recall though that the addition of F-buffer changes the ionic strength of the solution. This creates an osmotic gradient between the interior and exterior of the liposome. Even though there are K^+ ionophore molecules embedded in the membrane to provide K^+ ion access to the liposomes' internal compartments, a net loss of volume is anticipated with the addition of the high ionic strength solution. The cylinder fit yielded a large radial dimension, greater than ∼250 nm up to ∼335 nm and a length of ∼140 to ∼150

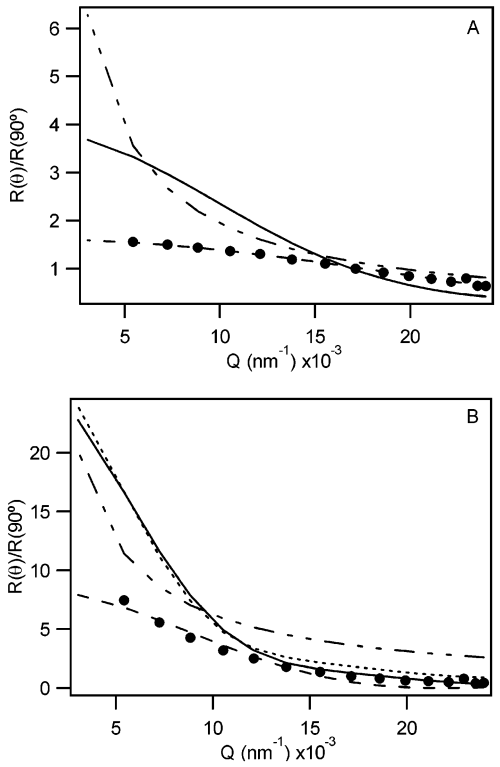

Figure 3. Light scattering spectra for plain liposomes in F-buffer at elution times of 32.867 and 40.55 min shown in frames A and B, respectively. Experimental observations are represented by the solid dots (●). The solid line represents the cylinder fit (—), the dashed—double-dotted line the thin rod fits (—··), the dashed line the thin spherical shell fit (- -), and the dotted line the thin disk fit (···). The thin disk fit overlaps the cylinder fit in part A.

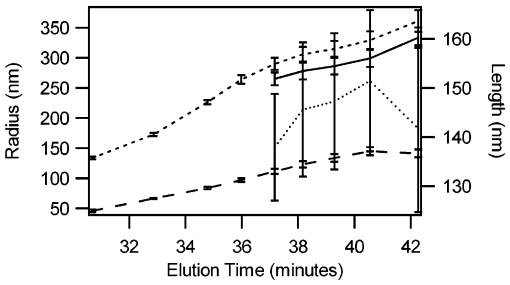

Figure 4. Physical sizing parameters for plain liposomes in F-buffer at nine representative times across the sample elution peak. Sizing parameters for three form factors are shown: the heavy dotted line represents the thin disk fit (•••), the dashed line represents the thin spherical shell fit (- -), and the cylinder fit is represented by the solid line (—) for its radial dimension and the lightly dotted line (···) for its length dimension (right axis).

nm; however, large errors were found in these determinations, exceeding 10%. The thin disk form factor showed an even greater radius than the cylinder and also showed larger errors than the thin spherical shell fit.

Plain liposomes in both G-buffer and F-buffer appeared to be similar in shape, while varying in size. Both can be considered spherical objects in light of the fact that the thin spherical shell fit had the lowest errors and that the cylinder fit gave dimensions that can be considered spherelike, in that the ratio of radius to length is on the order of 1. The variation in sizes was due to the osmotic gradients generated with the addition of high ionic strength solution.

Actin-Containing Liposomes in G-Buffer. Figure 5 shows MASLS spectra for actin-containing liposomes

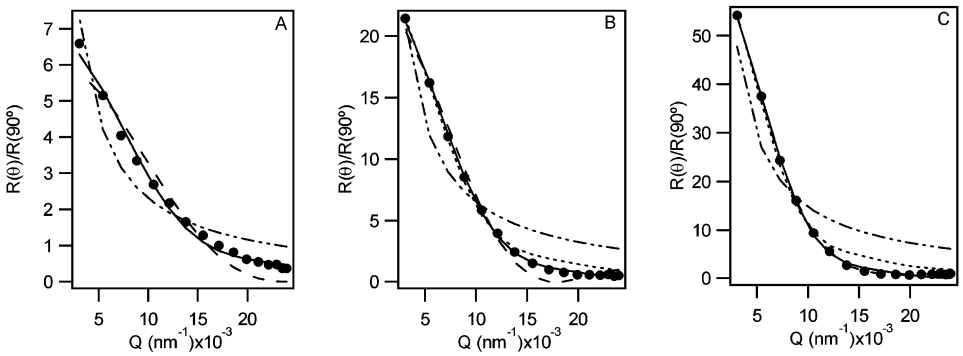

Figure 5. Light scattering spectra for actin-containing liposomes in G-buffer at elution times of 33.783, 36.267, and 38.033 min shown in frames A−C, respectively. Experimental observations are represented by the solid dots (●). The solid line represents the cylinder fit (—), the dashed−double-dotted line the thin rod fits (—••), the dashed line the thin spherical shell fit (- -), and the dotted line the thin disk fit (•••). The thin disk fit overlaps the cylinder fit in part A.

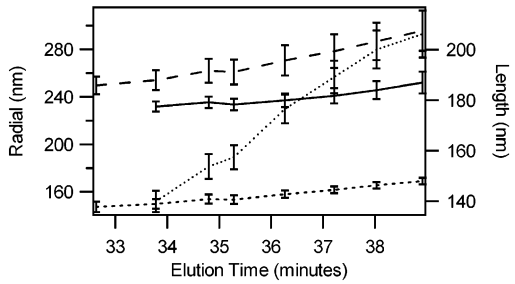

Figure 6. Physical sizing parameters for actin-containing liposomes in G-buffer at eight representative times across the sample elution peak. Sizing parameters for three form factors are shown: the heavy dotted line represents the thin disk fit (•••), the dashed line represents the thin spherical shell fit (- -), and the cylinder fit is represented by the solid line (—) for its radial dimension and the lightly dotted line (•••) for its length dimension (right axis).

produced via extrusion through a 400 nm pore diameter membrane in G-buffer. These experimental data are compared to the nonlinear least-squares fits of the four form factors. Panels A, B, and C show this for three different elution times. Panels A and B show the cylinder fit being the most accurate, with the thin spherical shell and thin disk displaying moderate accuracy. This is consistent with the trend for all early elution times. The thin rod fit did not appear to fit any of the time points in the elution peak. Late elution times did not show any model to be more accurate over all ranges of Q.

The fitted parameters followed a trend similar to that of the plain liposomes as is shown in Figure 6. The thin spherical shell fit yielded values of ∼150 to ∼160 nm radius with the smallest error of any of the fits, less than 3%. The cylinder had the next lowest errors and gave values of ∼230 to ∼240 nm radius with length dimensions varying from ∼150 to ∼200 nm and errors around 5%. Application of the thin disk model gave a radial dimension of ∼250 to ∼290 nm with errors of 7% to 8%. The thin rod model yielded parameters that had no physical significance. The shape that emerges from this investigation appears to be in the neighborhood of a 200 nm radius hollow spherical object. Both the thin shell and cylinder models support this in that application of the thin shell model reports a shell of ∼150 to ∼160 nm radius and the cylinder shows a cylindrical object with an aspect ratio on the order of 1.

Actin-Containing Liposomes in F-Buffer. Figure 7 shows the light scattering spectra for actin-containing liposomes produced by extrusion across a 400 nm diameter pore membrane in G-buffer, followed by polymerization in F-buffer. The figure shows the experimental data in comparison with the nonlinear least-squares fits for the four form factors. The four panels show the MASLS data at four different elution times along the dispersion elution peak. This set of spectra is unique in that it is the only occasion when the thin rod fit applied to the data in any significant way. This happened at very early elution times, before diverging from the experimental data at ∼33.5 min. The thin spherical shell fit never fit the data particularly well at any time during the elution peak. Both the thin disk and cylinder fits seemed to fit the data better than any of the other form factors, particularly at elution times greater than ∼34.7 min. The cylinder model in fact collapsed in the length dimension to its lower bound, while its radial parameter mimicked the thin disk radial parameter derived from the fitting procedure.

Figure 8 shows the physical sizing parameters obtained from the nonlinear least-squares fittings. One should quickly note that the parameters for the thin rod and cylinder fits are included only for portions of the elution peak. This too is true for the cylinder fit on the other sizing parameter plots. The reasoning behind the omission of the full fitted parameters is twofold. One reason is that the errors in some cases become so large as to render the values given insignificant. The other reason is that sometimes the values for the parameters obtained have no physical significance. The thin rod fitting returned values of between ∼200 and ∼500 nm with errors typically less than 10% in the portions of the peak where the fit was not overwhelmed by error. The thin spherical shell fit yielded radial parameters between ∼50 and ∼130 nm, with errors on the order of ±5%. The thin disk fit returned values for its radial parameter ranging from ∼75 nm early in the elution peak to ∼250 nm with errors not exceeding 5%. The cylinder fit mimicked the values of the thin disk for its radial dimension, with significant errors on the order of ±50%, while the length dimension collapsed to its lower bound of 13 nm with massive errors.

Discussion

The initial stages of this investigation were conducted to provide a control to which actin-containing liposomes could be compared. The plain G-buffer and F-buffer liposomes were investigated simply to confirm the known fact that these objects exist as spherelike assemblies. The light scattering spectra fit closely to the thin spherical shell fit and to the cylinder fit, which yielded parameters indicating thick "spherelike" shapes. These findings are plausible since empty liposomes in either G- or F-buffer should assume a spherical shape.

Actin-containing liposomes in G-buffer showed similar results derived from the fitting procedures implemented on empty liposomes. This experiment also provided a frame

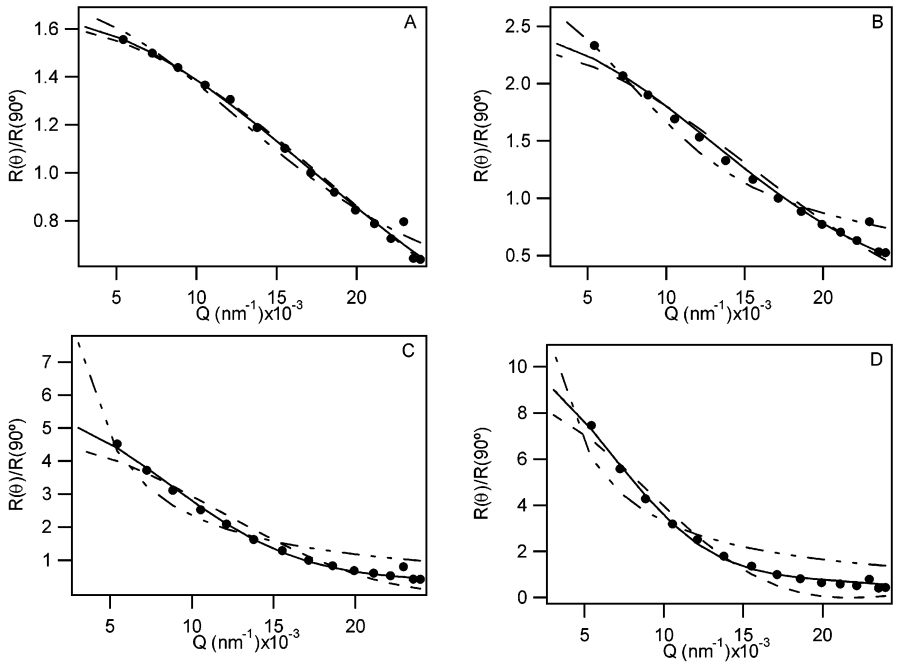

Figure 7. Light scattering spectra for actin-containing liposomes in F-buffer at elution times of 32.867, 34.783, 38.167, and 40.55 min shown in frames A−D, respectively. Experimental observations are shown as the solid dots (●). The solid line represents the cylinder fit (—), the dashed−double-dotted line the thin rod fit (—••), the dashed line the thin spherical shell fit (- -), and the dotted line the thin disk fit (•••). The thin disk fit overlaps the cylinder fit in parts A−D.

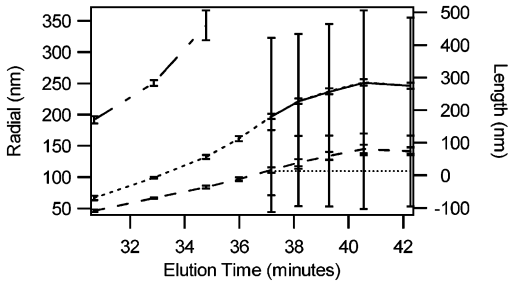

Figure 8. Physical sizing parameters for actin-containing liposomes in F-buffer at eight representative times across the sample elution peak. Sizing parameters for four form factors are shown: the heavy dotted line represents the thin disk fit (•••), the dashed line represents the thin spherical shell fit (- -), the dashed−double-dotted line represents the thin rod fit (—••) (right axis), and the cylinder fit is represented by the solid line (—) for its radial dimension and the lightly dotted line for its length dimension (•••) (right axis).

of reference for the actin-containing liposomes in F-buffer. These actin-containing liposomes in G-buffer are predicted to assume a spherical conformation similar to that of empty liposomes in G-buffer and F-buffer. Monomeric actin is not thought to have an effect on liposome conformation, and this was found to be the case. The physical sizing parameters for actin-containing liposomes in G-buffer were found to be comparable to the parameters for the empty liposome control runs in G- and F-buffer. On top of this, all fits showed similar trends to the empty liposome control runs across the sample peaks. The thin spherical shell fit, in particular, gave accurate spectral fitting and low errors in the parameters themselves. Hence, we conclude that actin-containing liposomes in low ionic strength buffers adopt a spherical shape. Our results are supported by similar observations reported by other groups studying giant actin-containing liposomes in low ionic strength buffer.[6−9] Some groups have observed that the presence of a charged bilayer is sufficient to induce actin polymerization on its surface.[17−19] We could not ascertain such phenomena with light scattering given the wavelength of the probing radiation. However, fluorescence microscopy of giant G-actin-containing liposomes do not show the presence of an actin cortex on the inner leaflet of giant liposomes.[8,9]

Analysis of actin-containing liposomes in F-buffer showed considerable differences from the control samples. First and foremost is the adoption of a thin disk conformation during the majority of the sample elution period. Another notable variation is the accuracy of the thin rod model for the early portions of the elution period. This is due to the fact that unencapsulated actin polymerizes into filaments, which are eluted first from the AFFF channel due to their extremely large aspect ratio, which results in low resistance to the cross flow. The numerical values of the length parameter are slightly low for standard actin filaments polymerized in vitro, 200−500 nm, but this is due to the fact that the filaments are subjected to shear forces, which can break their fragile structure. Another potential explanation is that these are indeed filaments, formed within liposomes which grew too large for the confines of the inner liposomal compartment and ruptured, releasing its content of 200−400 nm long F-actin filaments. It is clear from the spectra that the cylinder fit collapsed to its lower length dimension in an attempt to completely collapse to the calculated thin disk parameters. This results in large errors in the cylinder fit, while the thin disk fit shows a high level of correlation with the observed spectra and extremely low errors in the physical parameters.

The question now stands, why do actin-containing liposomes change conformation in high ionic strength solutions? The basis of this lies in the fact that the polymerizing actin filaments grow and push against the

(17) Rioux, L.; Gicquaud, C. *J. Ultrastruct. Res.* **1985**, *93*, 42−49.
(18) Laliberte, A.; Gicquanud, C. *J. Cell Biol.* **1988**, *106*, 1221−1227.
(19) Renault, A.; Lenne, P.-F.; Zakri, C.; Aradian, A.; Vénien-Bryan, C.; Amblard, F. *Biophys. J.* **1999**, *76*, 1580−1590.
(20) van Zanten, J. H. Characterization of Vesicles and Vesicular Dispersions via Scattering Techniques. In *Vesicles*; Rosoff, M., Ed.; Marcel Dekker: New York, 1996; pp 239−294.

inner membrane of the liposome. This pushing stretches the liposome causing other filaments to collapse into the region expanded by the stretching. This phenomenon differs from the situation in a eukaryotic cell, in that the liposome membrane has no anchor proteins to which the filaments can affix themselves. This results in the collapse of the natural and spontaneous three-dimensional filament network into what would be expected to be a disklike assembly.

Giant actin-containing liposomes, in which the G-actin has been polymerized into F-actin, have been found to undergo a variety of morphological changes, induced by the polymerization of actin. Häckl et al.[8] and Boulbitch et al.[9] observed the presence of a thin actin shell or cortex around the inside leaflet of the giant liposome after actin polymerization was induced via ionophore-mediated transport of salt across the liposome bilayer. It is important to note that these liposomes still retained their spherical shape. Miyata et al.[7] also observed the formation of a spherical assembly, after polymerization was initiated, with thin invaginations of lipid surrounding protrusive actin filaments emanating from the spherical body of the giant liposome. In contrast to these observations, Miyata and Hotani[6] observed the transformation of initially spherical actin-containing giant liposomes into either dumbbell or disklike shapes. This morphology was attributed to the formation of F-actin filaments and their arrangement into bundles. Our study has shown that polymerization of small actin-containing liposomes results in disklike structures. Our data agree well with Miyata and Hotani's[6] observation of actin-containing liposomes forming disklike shapes.

Conclusion

Submicrometer actin-containing liposomes in low ionic strength solutions were found to maintain a spherical configuration. However, when these actin-containing liposomes are exposed to high ionic strength solutions the liposomes were found to assume a thin disk shape. This was due to elongation of the developing actin filaments within the liposome's inner compartment.

Acknowledgment. We acknowledge support from the National Science Foundation BES-0196432.

LA035114D